

# Electromagnetic Comparison of 3-, 5- and 7-phases Permanent-Magnet Synchronous Machines : Mild Hybrid Traction Application

D. Ouamara <sup>a, b \*</sup>, F. Dubas <sup>a †</sup>, S.A. Randi <sup>c</sup>, M.N. Benallal <sup>b</sup>, C. Espanet <sup>d</sup>

<sup>a</sup> ENERGY Department, FEMTO-ST Institute, UMR CNRS 6174, UBFC, Belfort, France

<sup>b</sup> LESI Laboratory, University Djilali Bounaama of Khemis Miliana, Algeria

<sup>c</sup> Renault S.A., Guyanourt, France

<sup>d</sup> UBFC, Belfort, France

## ARTICLE INFO

### Article history :

Received July 2016

Accepted September 2016

### Keywords :

Energy balance ;

Harmonic analysis ;

Numerical ;

Permanent-magnet ;

Synchronous Machines ;

Star of slots.

## ABSTRACT

Authors compare the electromagnetic performances of three multi-phases permanent-magnet (PM) synchronous machines (PMSM) for Mild Hybrid-traction application. This comparison was made using two-dimensional (2-D) numerical simulations in transient magnetic with eddy-current reaction field in the PMs. The best machine was determined using an energetic analysis (i.e., losses, torque and efficiency) according specifications. In this study, the non-overlapping winding with double layer (i.e. all teeth wound type) was used. The winding synthesis is based on the "Star of slots" method as well as the Fourier series decomposition of the magnetomotive force (MMF).

©2016 LESI. All rights reserved.

## 1. Introduction

The humanity energy consumption has generally been growing. The latter is accompanied by emission of greenhouse gases. In this context, the automotive sector, which represents about a third part of the overall world energy consumption, may well evolve to become a contributor to reduction of emissions by developing and selling hybrid vehicles. Depending on the degree of hybridization, which corresponds to the quantity of power that can provide the electrical energy source compared to fossil energy source, different types of drive have been developed [1] :

- Full Hybrid : combination of a combustion engine and an electric motor, the latter

\*Email : daoud.ouamara@gmail.com

†Email : fdubas@gmail.com

provide a power more than 30 % of the total power. The electric motor is rather used for low-speed operation, while the combustion engine is used at high-speed.

- Mild Hybrid :the part of electric motor is between 10 % and 30 % of the total power. This version is equipped by a kinetic energy recovery system, consisting of electrical machine in the generator operating mode. Contrary to the Full Hybrid, the electric motor is only used to assist the vehicle during the acceleration phases.
- Micro Hybrid :it is not strictly a hybrid. Known as "Stop & Start",it ensures a modest electric energy consumption andreduction of CO2 emissions. At stop, the combustion engine shuts down and restart when the accelerator is pushed. The electric part is less than 10 % of the total power.

In this article, we are considering only electric motorization of Mild Hybrid powertrain.

The studied electrical machinesaremulti-phases (3-phases included) surface-mounted PMSMwith concentrated all teeth wound (two layers) winding. This topology of machines is assumed to be a good candidate for this kind of application : good torque density, lower maintenance costs, and simple construction . . . [2-3]. In addition to advantages associated to this structure, the multi-phase system ensure operation in degraded mode if phase's number is greater than 3, which is a powerful asset in automotive traction [4-7]. The comparison via an energy balance will be carry out considering three electrical machines :

- **Machine A** : 12-slots/10-poles/3-phases ;
- **Machine B** : 20-slots/18-poles/5-phases ;
- **Machine C** : 28-slots/26-poles/7-phases.

**Machine A** is well known in literature [8]. From this topology, **Machine B** and **Machine C** are deduced. It should be noted that **Machine B** was studied in [9].The comparative study of those machines will be subdivided into two parts, namely :

- The winding analysis based on the "Star of slots" method as well as the Fourier series decomposition : winding distribution, MMF waveform and winding factor ;
- and the electromagnetic numerical modeling, viz., electromagnetic torque, torque ripple, back electromotive force (EMF), in order to compare the machines via an energy balance (i.e., iron/copper/PMs losses and efficiency).

The terms of reference for this comparative study are :

- Identical mass ;
- Dimension :  $D_{ex} = 138.4 \text{ mm}$  and  $L_z = 136 \text{ mm}$  ;
- Rotating speed : 3,000 rpm.

## 2. Winding Synthesis

Fig. 1 represents the topology of the machines and the spatial distribution of various phases. The phases of winding are star-connected and the studied machines are supplied by sinusoidal current. The direction of PMs magnetization is supposed to be radial.

Machines that have  $2p = N_d \pm 2$  (where  $p$  and  $N_d$  are respectively the pole pairs and slots number) are generally characterized by low detent torque [10]. Consequently, the number of poles chosen is : 18 poles for **Machine B** (with 20 teeth) and 26 poles for **Machine C** (with 28 teeth).

In order to synthesize a winding with higher performances, the "star of slots" method

is used [11-12]. The phases distribution of the machines via this method is defined on Fig. 2.

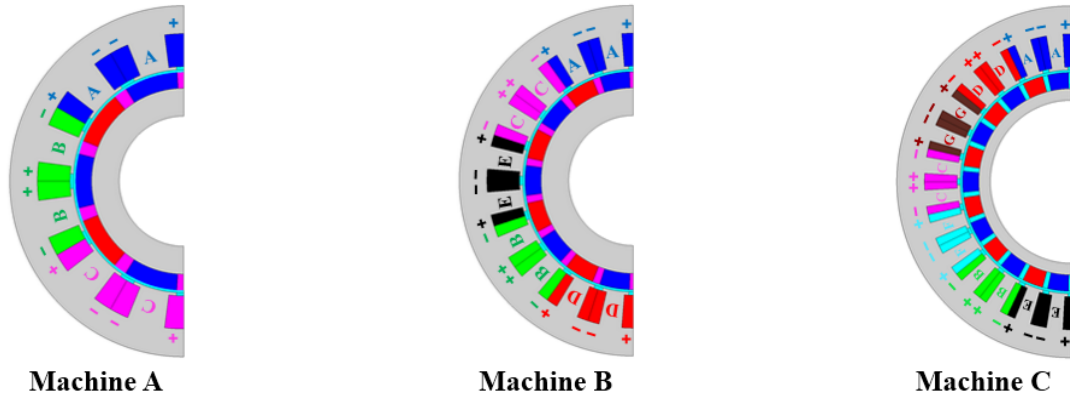


Fig. 1 – Description of machines : Topology & Winding distribution.

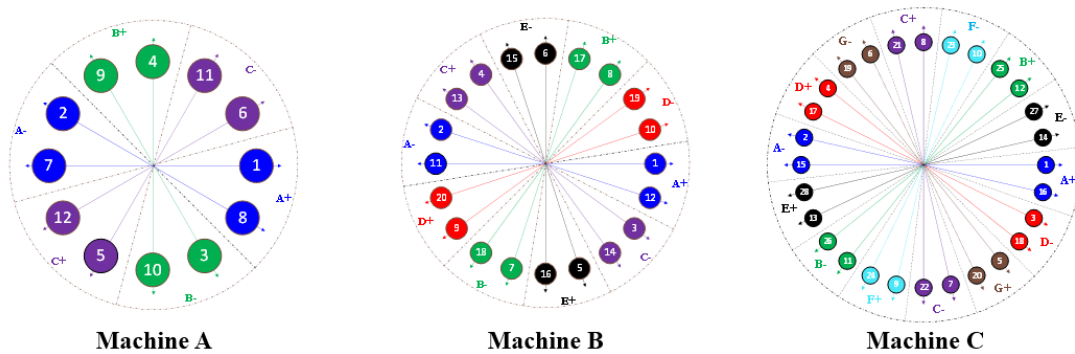
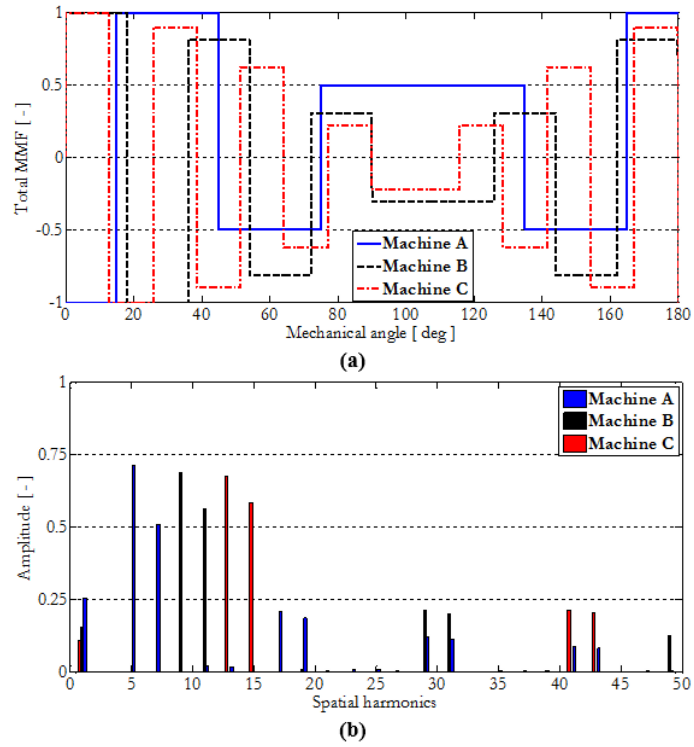
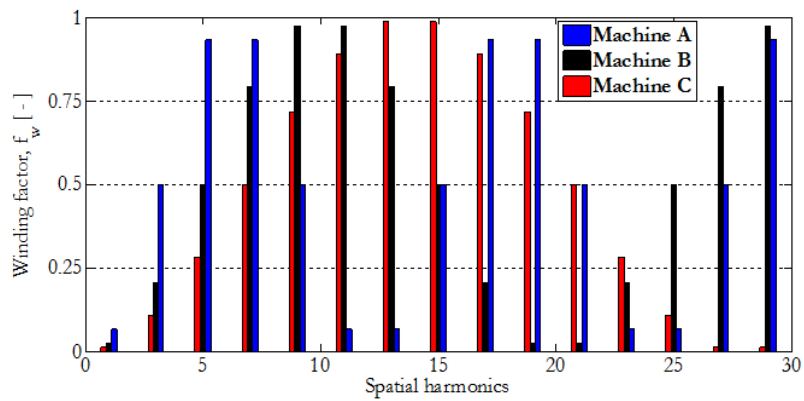


Fig. 2 – Distribution of phases via the "Star of slots" method.

Fig. 3 shows the pattern of total MMF [see Fig. 3(a)] and its corresponding harmonic spectrum [see Fig. 3(b)] of the two layers concentrated winding of the machines. Spatial harmonics spectrum shows the 5th harmonic order is higher than fundamental for the **Machine A**, 9<sup>th</sup> for the **Machine B** and 13th for the **Machine C** that confirms our choice about poles number of machines studied.



**Fig. 3** – Total MMF : (a) Waveform and (b) Harmonic spectrum.



**Fig. 4** – Winding factor.

Another element of significant importance is the winding factor, and it will be calculated. The calculation of this latter will be done by comparing MMF harmonics of the studied winding [see Fig. 1], by Fourier series decomposition, with harmonics of the diametric winding associated. Fourier series decomposition of studied and diametric winding is given by :

$$\varepsilon = \sum_{k=1}^{\infty} \frac{NI}{k\pi} \cdot A_k^* \cdot \cos(k \cdot \theta) \quad (1)$$

with  $N$  the number of turns,  $I$  the RMS current, and

$$A_k^e = \sin\left(\beta^+ \cdot \frac{k\pi}{2}\right) + \sin\left(\beta^- \cdot \frac{k\pi}{2}\right) - 2\sin\left(\frac{k\pi}{2}\right) \quad (2)$$

for the studied winding with  $\beta^\pm = ((m \pm 1))/m$  where  $m$  is the number of phases, and

$$A_k^d = 2 \cdot \left\{ 1 - \sin\left[(1 - 2k) \cdot \frac{\pi}{2}\right] \right\} \quad (3)$$

for the diametric winding.

The winding factor is calculated by  $f_w = |A_k^e| / |A_k^d|$  (estimated between 0 and 1) and results of calculation are given on Fig. 4; whose winding factor is equal to 0.933 for **Machine A**, 0.9875 for **Machine B**, and 0.9755 for **Machine C**. Even harmonics have a winding factor null. The periodicity of the winding factor is equal to  $N_d$  for the studied machines [see Fig. 4].

In conclusion of this part, the choice of poles number of studied machines is consistent with obtained results. The 5<sup>th</sup>, 9<sup>th</sup> and 13<sup>th</sup> harmonics order of **Machine A**, **Machine B** and **Machine C** respectively, are characterized by higher amplitudes in Fourier series decomposition of MMF and by higher winding factor. Notice that we could have also chosen 7 pole pairs for **Machine A**, 11 pole pairs for **Machine B** and 15 pole pairs for **Machine C**. In order to have a lower frequency, the first choice was selected for the comparative study.

### 3. 2-D Numerical Simulation

The comparison via an energy balance is performed using 2-D numerical simulations in transient magnetic with taken into account eddy-current reaction field in the PMs[13]. For the studied machines, the magnetic steel M270-35A of Arcelor Mittal has been considered. The PMs type is N37H whose remanent flux density is equal to 1.1 T at 100 °C. No-load/Load simulations will determine the back EMF, the electromagnetic torque as well as the torque ripple, the iron/copper/PMs losses and the efficiency.

Fig. 5 represents the distribution map of magnetic flux densities in the three machines. It should be noticed that the maximum value of magnetic flux density in the teeth reach 1.6 T for **Machine A**, 1.4 T for **Machine B**, and 1.2 T for **Machine C**; while in the tooth-tips, the magnetic material is saturated. It is due to the fact that surface tip is not large.

Fig. 6 shows the electromagnetic torque and torque ripple for the three machines. Considering weakness of torque ripple, the cogging torque is neglected. The mean value of electromagnetic torque is 71.5 Nm, what satisfy the requirements specification. The torque ripple rate is defined by

$$\Delta T_{em} (\%) = \frac{T_{em_{max}} - T_{em_{min}}}{T_{em_{moy}}} \times 100 \quad (4)$$

It should be noted that ripple value is less than 1 % for Machine B and Machine C.

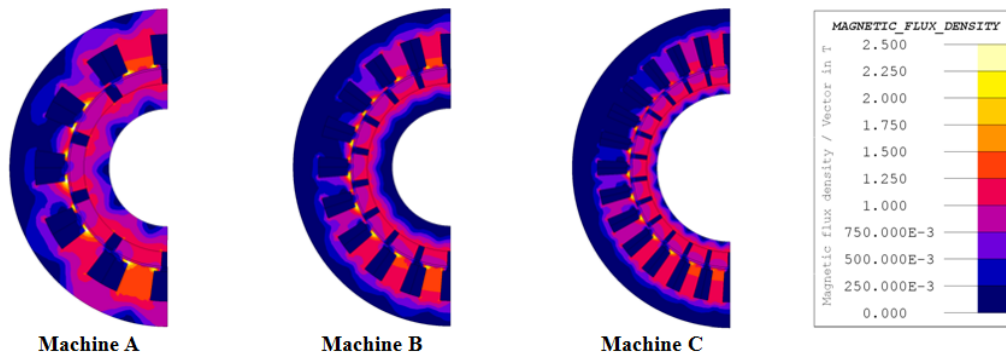


Fig. 5 – Distribution map of magnetic flux densities.

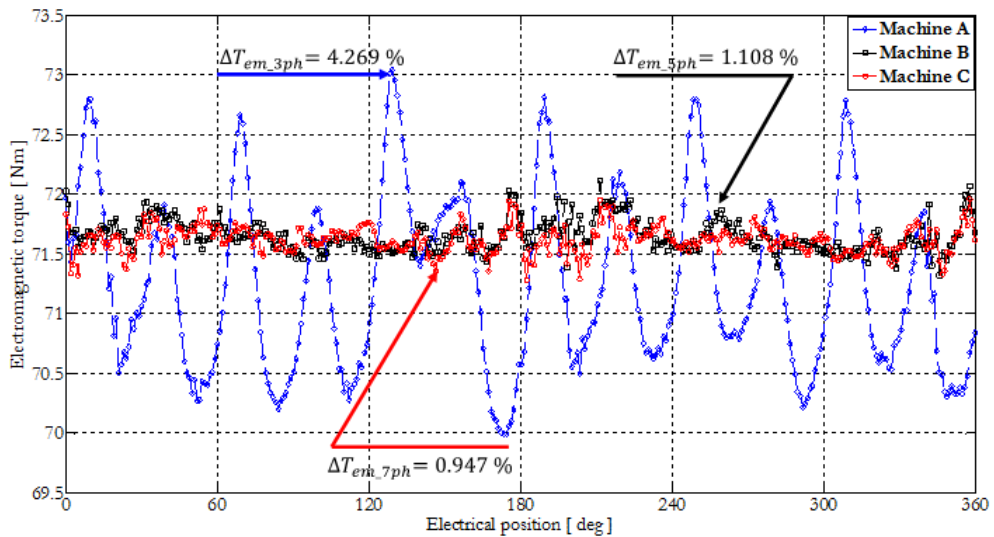
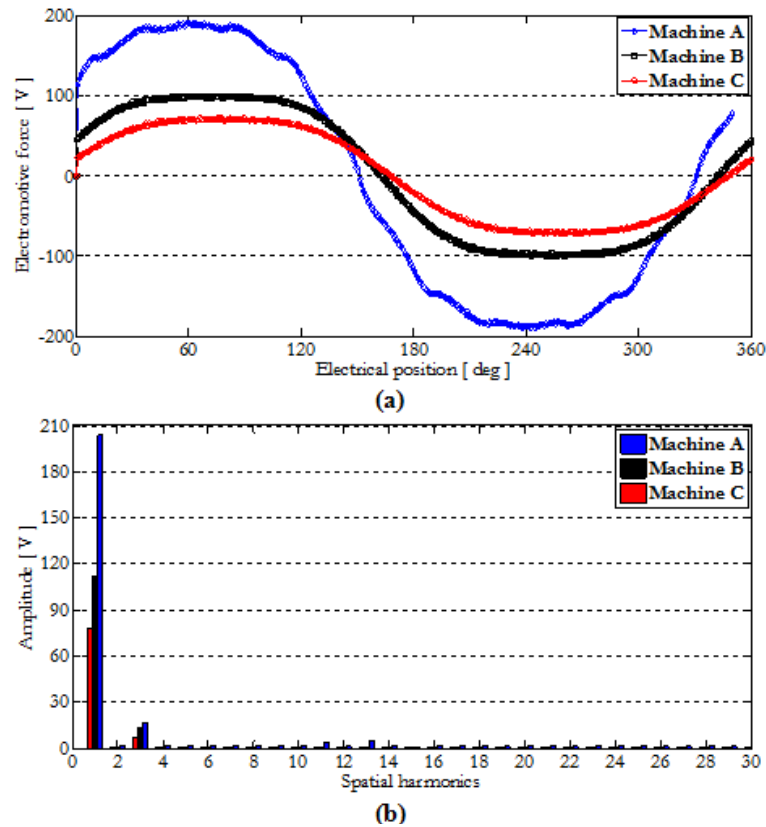


Fig. 6 – Electromagnetic torque.



**Fig. 7** – Back EMF : (a) Waveform and (b) Harmonic spectrum.

Fig. 7 shows the back EMF waveform of phase A at no-load [see Fig. 7(a)] as well as the harmonic spectrum [see Fig. 7(b)]. **Machine A** has a higher amplitude against **Machine B** and **Machine C** respectively.

To estimate the PM eddy-current losses, the electrical circuit used for simulation is represented in Fig. 8. Based on Kirchhoff's current law in the  $\sum I = 0$  form, no current flowing outside the PM should be provided. In order to take into account the eddy-current reaction field, each PM has been modeled as a solid conductor (i.e., SC1-SC2) with a high value resistance ( $\approx 10^9 \Omega$ ) at the ends of the PMs (i.e., R6-R7) in the electrical circuit. Without the eddy-current reaction field, the solid conductive regions in the electrical circuit are not necessary. It can be noted that the PMs are finely meshed (i.e., more than three elements in the skin depth of the PMs) to take into account the skin effect [14]. The mesh has been optimized so that the PMs eddy-current losses can converge numerically. The PMs eddy-current losses for the three machines are illustrated in Fig. 9. **Machine B** is better than its counterparts in terms of PMs eddy-current losses.

The DC copper losses (i.e., without the skin effect) in the windings at  $I = 30$  are 108 W for **Machine A**, 180 W for **Machine B**, and 252 W for **Machine C**. The increase of the phase's number causes additional losses.

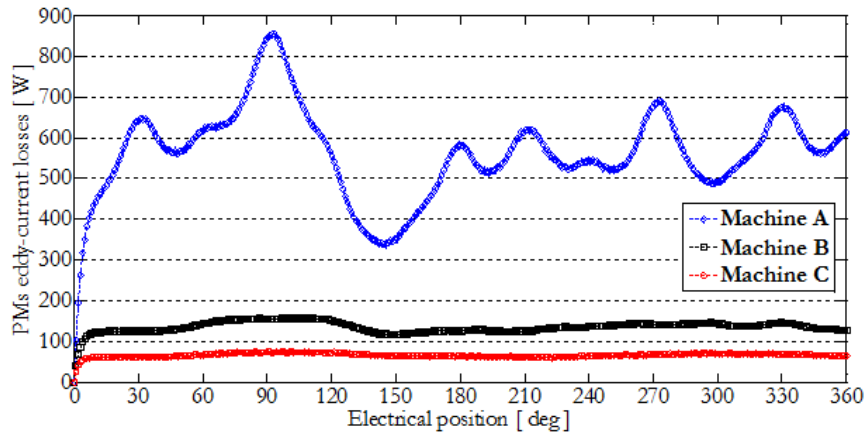


Fig. 8 – PMs eddy-current losses.

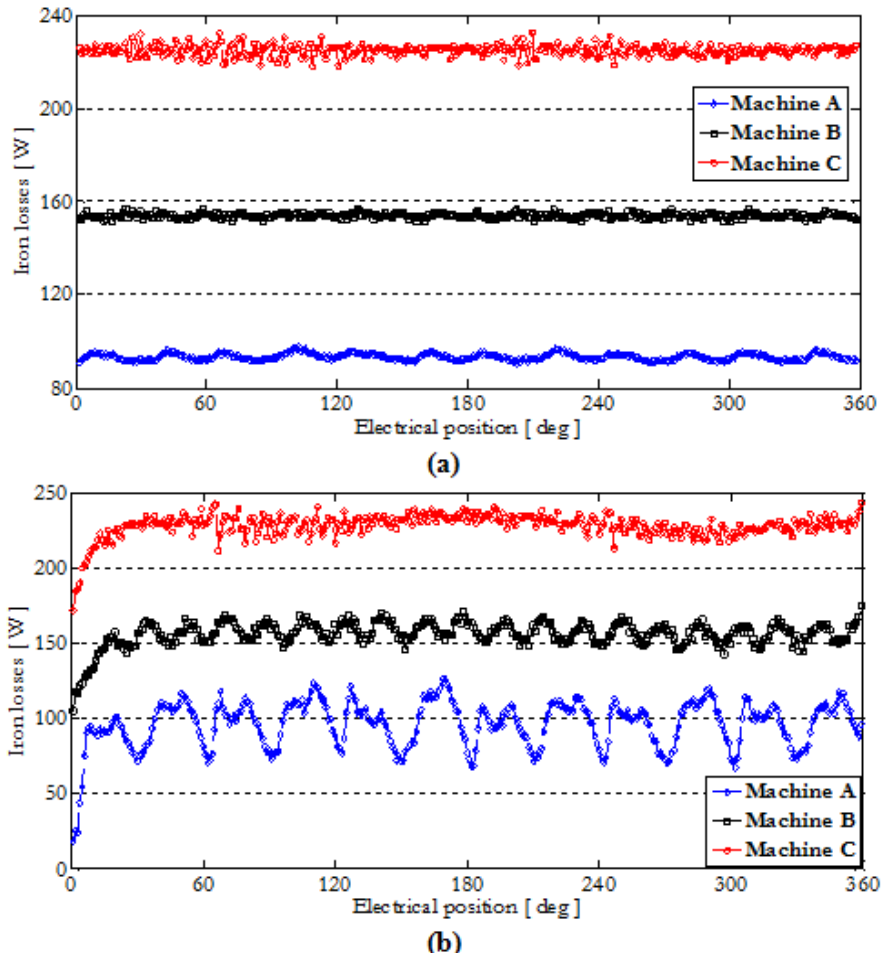


Fig. 9 – Iron losses : (a) Bertotti method, and (b)LS module.

Iron losses are separated on three types of losses : i) hysteresis, ii) eddy-current, and iii) excess. Those magnetic losses are determined numerically from Bertotti method [15] and with using “Loss Surface” (LS) module [16]. Various losses per volume, defined by Bertotti method, are given by :

$$dP_H = K_h B_m^2 f \quad (\text{Hysteresis}) \quad (5)$$

$$dP_J = \frac{\pi^2 \sigma d^2}{6} (B_m f)^2 \quad (\text{Eddy - current}) \quad (6)$$

$$dP_E = 8,67.K_e (B_m f)^2 \quad (\text{Excess}) \quad (7)$$

**Table 1** – Data of the sheet M270-35A (Bertotti Method).

Designation	Symbols	Machine A	Machine B	Machine C
Volumetric mass density	$\rho$		7650 $Kg.m^{-3}$	
Electrical conductivity	$\sigma$		$1.92 \times 10^6 S.m^{-1}$	
Thickness	$d$		0.35 mm	
Hysteresis coef.	$K_h$	123.313	126.12	128.686
Excessive coef.	$K_e$	0.739	0.738	0.739

**Table 2** – Summary of the comparison.

	Machine A	Machine B	Machine C
Slots number	12	20	28
Phases number	3	5	7
Poles number	10	18	26
Winding	Concentrated all teeth wound (two layers)		
Outside diameter		138.4 mm	
Iron length		136 mm	
Total volume		1.615 L	
Rotation speed		3,000 rpm	
Torque		71.5 Nm	
DC copper losses	108 W	180 W	252 W
PMs eddy-current losses	561.4 W	134.42 W	74.44 W
Iron losses (LS)	96.7 W	156.45 W	228.55 W
Iron losses (Bertotti)	93.36 W	153.86 W	224.8 W
Output power		22.45 kW	
Efficiency	96.3 %	97.29 %	96.6 %

The physical parameters and the coefficients are given in Table 1 for M270-35A sheet. Fig. 10 represents the iron losses with Bertotti method [see Fig. 10(a)] and LS module. [see Fig. 10(b)]. As that magnetic losses are linked to magnetic flux density and to frequency, it is clear that **Machine C** will have more losses than **Machine B** and **Machine A** respectively. The flux density value of the three machines are close, so the frequency is the element causing the difference in magnetic losses. Results of this study are summarized in Table 2 with the calculation of efficiency of suited machines.

#### 4. Conclusion

This comparative study is a part of modeling and design of multi-phases PMSMs. It is shown that for same quantities of iron/copper/PMs losses, torque ripple is less important for **Machine B** (5-phases) and **Machine C** (7-phases) in comparison with **Machine A** (3-phases), and it is obtained for the same average electromagnetic torque.

At end of this study, **Machine C** is more suitable by having less PMs eddy-current losses against **Machine B** and **Machine C**. Iron losses are more important in **Machine C** due to poles number, which is, greater than the two others studied machines. However, the machine having 5-phases, may be interesting in terms of control (less complicated against the one having 7-phases). **Machine A** is not selected because of important PMs eddy-current losses and torque ripple in comparison with **Machine B** and **C**.

Different outlooks may be considered, viz., a comparative study for different PMs disposals, magnetization direction or other windings patterns.

#### Acknowledgements

This work is supported by RENAULT-SAS, Guyancourt, France.

#### REFERENCES

- [1] C.C. Chan, A Bouscayrol, K. Chen, « Electric, Hybrid and fuel Cell Vehicles : Architectures and Modelling », IEEE Transactions on Vehicular Technology, vol. 59, no. 2, pp. 589-598, 2010.
- [2] J. Wang, X. Yuan, K. Atallah, « Design Optimization of a Surface-Mounted Permanent-Magnet Motor With Concentrated Windings for Electric Vehicle Applications », IEEE Transactions on Vehicular Technology, vol. 62, no. 3, pp. 1053-1064, 2013.
- [3] A. Cassat, C. Espanet, R. Coleman, L. Burdet, E. Leleu, D. Torregrossa, J. M'Boua, A. Miraoui, « A Practical Solution to Mitigate Vibrations in Industrial PM Motors Having Concentric Windings », IEEE Transactions on Industry Applications, vol. 48, no. 5, pp. 1526-1538, 2012.
- [4] E. Levi, « Multiphase Electric Machines for Variable-Speed Applications », IEEE Transactions on Industrial Electronics, vol. 55, no. 5, pp. 1893-1909, 2008.
- [5] K.T.J.E. Miller, M.I. McGilp, « Analysis of Multi-Phase Permanent-Magnet Synchronous Machines », International Conference on Electrical Machines and Systems, ICEMS 2009, Tokyo (Japan).
- [6] L. Parsa, H.A. Toliyat, « Five-Phase Permanent-Magnet Motor Drives », IEEE Transactions on Industry Applications, vol. 41, no. 1, pp. 30-37, 2005.

- [7] F. Scuiller, J-F. Charpentier, E. Semail, S. Clénet « Comparison of two 5-phase Permanent Magnet machine winding configurations. Application on naval propulsion specifications », IEEE International Electric Machines & Drives Conference, IEMDC 2007, Antalya (Turkey).
- [8] I. Petrov, P. Ponomarev and J. Pyrhönen, « Torque ripple reduction in 12-slot 10-pole fractional slot permanent magnet synchronous motors with non-overlapping windings by implementation of unequal stator teeth widths », International Conference on Electrical Machines, ICEM 2014, Berlin (Germany).
- [9] B. Aslan, E. Semail, J. Korecki and J. Legranger, « Slot/pole combinations choice for concentrated multiphase machines dedicated to mild-hybrid applications », 37th Annual Conference on IEEE Industrial Electronics Society, IECON 2011, Melbourne (VIC).
- [10] A. Soualmi, F. Dubas, A. Randria, C. Espanet, « Comparative Study of Permanent-Magnet Synchronous Machines with Concentrated Windings for Railway Application », International Conference on Electrical Machines and Systems, ICEMS 2011, Beijing (China).
- [11] N. Bianchi, M. Dai Pré, « Use of the Star of Slots in Designing Fractional-Slot Single-Layer Synchronous Motors », IEE Proceedings-Electric Power Applications, vol. 153, no. 3, pp. 459-466, 2006.
- [12] M. Hörz, H-G. Herzog, A. Haas, « Axial Flux Machine with Single Tooth Fractional Slot Winding – Comparaison of Different Winding Design Approaches », International Symposium on Power Electronics, Electrical Drives, Automation and Motion, SPEEDAM 2006, Taormina (Italy).
- [13] Flux2D, « General operating instructions – Version 12.1. », Cedrat S.A. Electrical Engineering, 2015, Grenoble, France.
- [14] F. Dubas, A. Rahideh, « Two-Dimensional Analytical Permanent-Magnet Eddy-Current Loss Calculations in Slotless PMSM Equipped With Surface-Inset Magnets », IEEE Transactions on Magnetics, vol. 50, no. 3, 6300320, 2014.
- [15] G. Bertotti, « General properties of power losses in soft ferromagnetic materials », IEEE Transactions on Magnetics, vol. 24, no. 1, pp. 621-630, 1988.
- [16] T. Chevalier, A. Kedous-Lebouc, B. Comut, « A new dynamic hysteresis model for electrical steel sheet », Physica B : Physic of Condensed Matter, vol. 275, no. 1-3, pp. 197-201, 2000.